Chemosphere 75 (2009) 193–199

Contents lists available at ScienceDirect

Chemosphere

journal homepage: www.elsevier.com/locate/chemosphere

Microarray-based functional gene analysis of soil microbial communities during ozonation and biodegradation of crude oil

Yuting Liang [a,b], Joy D. Van Nostrand [b,c,1], Jian Wang [a], Xu Zhang [a], Jizhong Zhou [b,c,1], Guanghe Li [a,*]

[a] Department of Environmental Science and Engineering, Tsinghua University, Beijing 100084, China
[b] Institute for Environmental Genomics and Department of Botany and Microbiology, University of Oklahoma, Norman, OK 73019, USA
[c] Virtual Institute for Microbial Stress and Survival

ARTICLE INFO

Article history:
Received 29 September 2008
Received in revised form 3 December 2008
Accepted 4 December 2008
Available online 13 January 2009

Keywords:
GeoChip
Microbial communities
Functional genes
Ozonation
Biodegradation

ABSTRACT

Ozonation with a subsequent biodegradation treatment was performed to remove recalcitrant organic compounds from long-term weathered crude oil contaminated soil. Samples were analyzed by GC/MS and column chromatography to monitor changes in crude oil composition. A functional gene array was used to examine microbial community dynamics. After a 6 h ozonation treatment with a constant concentration of 10 mg O_3 L^{-1} at a flow rate of 2.0 L min^{-1}, an average removal of crude oil was 22%. The concentration of long-chain *n*-alkanes (C_{19}–C_{28}) decreased while more biodegradable short-chain alkanes (C_{14}–C_{16}), *n*-aldehydes (C_{13}–C_{20}), and *n*-monocarboxylic acids (C_9–C_{20}) appeared. In the subsequent direct biodegradation and bioaugmentation, an additional 12–20% of residuals were removed. The total microbial functional gene numbers and overall genetic diversity decreased after ozonation. Also, most of the key functional genes pertaining to carbon, nitrogen, and sulfur cycling and organic contaminant degradation decreased, ranging from 20% to below the detection limit. However, in the subsequent biodegradation treatments, with and without bioaugmentation, the abundance of key genes in most functional groups recovered. This study provided insight into changes in crude oil composition and microbial functional genes responses during ozonation and bioremediation treatments. These changes demonstrate the feasibility of an integrated ozonation and biodegradation treatment to remove recalcitrant soil contaminants.

1. Introduction

Crude oil is a complex mixture composed of mainly *n*-alkanes, aromatic hydrocarbons and non-hydrocarbon compounds, such as polar fractions with hetero-atoms of nitrogen, sulfur and oxygen (NSO fraction), and asphaltenes. While crude oil is arguably the most important resource in modern history, crude oil contamination has become a critical issue as a result of releases during exploration, production, maintenance, transportation, storage and accidents, causing significant environmental impacts and presenting a substantial threat to human health.

Largely due to low levels of the nutrients nitrogen and phosphorus, low abundance and activity of hydrocarbon-degrading bacteria, aging and sequestration of contaminants to soil pores, natural attenuation of complex components of crude oil (e.g. long-chain alkanes, polycyclic aromatic hydrocarbons (PAHs), branched and alicyclic hydrocarbons) occurs very slowly (Romantschuk et al., 2000; Semple et al., 2003; Ivancev-Tumbas et al., 2004). However, even under optimum environmental conditions (i.e., nutrient amendments, aeration, moisture, temperature and pH control), high-molecular weight compounds with complex structures, the majority of residual contaminants, show minimal degradation via bioremediation, especially at heavily-polluted, historically-contaminated sites (Chaineau et al., 1995; Huesemann, 1995; Angehrn et al., 1998; Nocentini et al., 2000; Ivancev-Tumbas et al., 2004).

Chemical oxidation can be used to remove recalcitrant contaminants (e.g. PAHs, chlorinated solvents, and pesticides) in soil and groundwater (Rivas, 2006; Ferrarese et al., 2008; Sung et al., 2008). Compared to other oxidants like Fenton's reagent, permanganate, and persulfate, ozone gas is advantageous because of its higher diffusivity into soil. The oxidation process occurs both by direct ozone molecular oxidation and indirect oxidation of transient secondary oxidant species including hydroxyl (·OH), perhydroxyl ($HO_{2}\cdot$), superoxide (O_2^{-}), and ozonide (O_3^{-}) radicals. The indirect oxidation process is non-selective and can be promoted by metal oxides (e.g., Fe, Mn oxide) and humic substances in the soil. The products of ozonation include CO_2, H_2O, and additional biodegradable intermediates such as alcohols, ketones, and carboxylic acids. Thus it may be possible to integrate ozonation and bioremediation

* Corresponding author. Tel.: +86 10 627 73232; fax: +86 10 627 85687.
E-mail address: ligh@tsinghua.edu.cn (G. Li).
[1] http://vimss.lbl.gov.

0045-6535/$ - see front matter © 2008 Elsevier Ltd. All rights reserved.
doi:10.1016/j.chemosphere.2008.12.007

Table 1
Physico-chemical characteristics of soil samples collected from Daqing oilfield.

Parameters	Values
Texture	Clay 0.6%, silt 24.7%, fine sand 41.1%, coarse sand 33.6%
pH	7.3
Water content (wt%)	5.9
Available phosphorus (mg kg^{-1})	11.0
Available nitrogen (mg kg^{-1})	11.1
Humus (mg g^{-1})	11.8
Total Fe (mg kg^{-1})	25.0
Total Mn (mg kg^{-1})	36.6

to remove organic contaminants from soil (Nam and Kukor, 2000; Kulik et al., 2006; O'Mahony et al., 2006).

An important question concerning the combination of ozonation and biodegradation is the potential lethal effects of ozonation on indigenous microbial populations as ozone is a strong sterilizing agent. It has been reported that ozonation substantially decreases microbial populations with ozonation time (Jung et al., 2005), and that additional consortia or specific inoculations of bacteria have to be used to further degrade the contaminants (Nam and Kukor, 2000; O'Mahony et al., 2006). However, the impact of chemical oxidation on indigenous microbial communities and the subsequent dynamics of both surviving and inoculated microbes have not been well studied.

The rapid development of genomic tools has greatly advanced the knowledge of microbial communities in complex environments. In order to better understand the diversity and functions of microbial communities, GeoChip, a robust functional gene array, containing 24,243 oligonucleotide probes covering >10,000 genes in >150 functional groups involved in nitrogen, carbon, and sulfur cycling, metal reduction and resistance, and organic contaminant degradation, was developed (He et al., 2007). The GeoChip has been shown to be a high-throughout and powerful genomic technology for investigating biogeochemical, ecological and environmental processes (Rhee et al., 2004; Li et al., 2005; He et al., 2007; Yergeau et al., 2007; Wu et al., 2008; Zhou et al., 2008).

In this study, a laboratory-scale soil ozonation with subsequent biodegradation experiment was carried out. GC/MS and column chromatography were used to follow the contaminant composition, and GeoChip was used to profile the microbial functional gene changes after ozonation and in the subsequent biodegradation treatments with and without bioaugmentation. The results indicated that most of the microbial functional genes represented a high capacity for recovery and adaptation after a decrease during the ozonation phase.

2. Materials and methods

2.1. Soil sample and physico-chemical characteristics

Crude oil contaminated soil samples were taken at 5–20 cm depth from the Daqing oilfield, northeast China, where contamination has occurred for more than 10 years. The soil was sealed in sterile sampling bags and transported to the lab on ice. To compare the compositional change in subsurface extracted crude oil and soils, crude oil was also taken from a pumping well. Indigenous microbes were enriched from 5 g contaminated soil in 100 mL minimal salts medium with paraffin as the sole carbon source in a flask (250 mL) with shaking (50 rpm) at 30 °C. Once the hydrocarbon-degrading bacterial population reached 10^7 cells mL^{-1}, the culture was inoculated into contaminated soil (30 mL kg^{-1} soil). The soil was incubated for 242 d and was stirred twice a week for aeration. Environmental conditions were controlled as follows: temperature 18–25 °C, water content 10–20%, pH 6.5–7.0 and nitrogen and phosphorus supplement with urea and phosphate at a C/N/P ratio of 100:10:1. Since large amounts of residual contaminants were still detectable after the 242 d incubation, the soil was used for further ozonation with subsequent biodegradation experiments to remove recalcitrant contaminants.

The physico-chemical characteristics of the soil before ozonation treatment were determined (Lu, 1999) (Table 1). Soil water content was measured by drying 10–20 g soil at 105 °C for 8 h. Soil pH was measured in a 1:2.5 mixture of soil/water (0.01 M $CaCl_2$ solution) with a pH electrode. Available phosphorus was measured in 0.5 M $NaHCO_3$ extraction solution (pH 8.5) using a molybdenum–antimony colorimetric method. Available nitrogen was measured by the MgO-alloy distillation method. Loose and steady humus was measured by NaOH and sodium pyrophosphate extraction. Available micronutrients (Fe and Mn) were determined with inductively coupled plasma atomic emission spectrometry (Yu et al., 2001).

2.2. Ozonation system

A schematic of the laboratory-scale soil column experimental system is illustrated in Fig. 1. The system was composed of an ozone generator, three soil columns (approximately 300 g soil in each column), ozone and CO_2 measurement devices, and a residual gas absorption device. The ozone generator (JS-10, Jinshuo Company) used air to produce oxygen, which was then transformed to ozone by glow discharge with a maximum performance of 10 g O_3 h^{-1}. The soil column was made of organic glass with an inner diameter of 60 mm and a height of 350 mm. Ozone flowed into the bottom of the column and distributed evenly via a porous organic glass plate. The flow rate was adjusted with a flowmeter. Outlet gas flowed into a NaOH solution (0.2 M) to absorb CO_2. When measuring the ozone concentration, the gas flow direction was redirected into a KI solution (20% w/w) and an aliquot of gas (2 L) was taken with a rotameter. A water column (1 m in height) was set up in case all valves were closed. Residual gas flowed into a $Na_2S_2O_3$ solution (approximately 0.1 M).

To measure the concentration of CO_2, an aliquot (2 mL) of NaOH solution which had reacted with outlet gas was collected. Supersaturated $BaCl_2$ solution (1 M) was added to precipitate Na_2CO_3 and the residual NaOH was titrated with HCl (0.1 M), using phenolphthalein as the indicator. The concentration of ozone was measured by adding H_2SO_4 [5 mL, 1:5 (H_2SO_4:H_2O)] to an aliquot of gas (2 L) immediately following flow through the absorption flask. The gas/H_2SO_4 mixture was shaken and incubated for 5 min and then titrated with a $Na_2S_2O_3$ solution (0.1 M) until the color changed to a light yellow. Amylum solution (1 mL) was added and then titrated with a $Na_2S_2O_3$ solution until colorless.

2.3. Biodegradation system

After ozonation, soils were taken from the ozonation system and mixed thoroughly. Aliquots of the ozonated soil (540 g) were

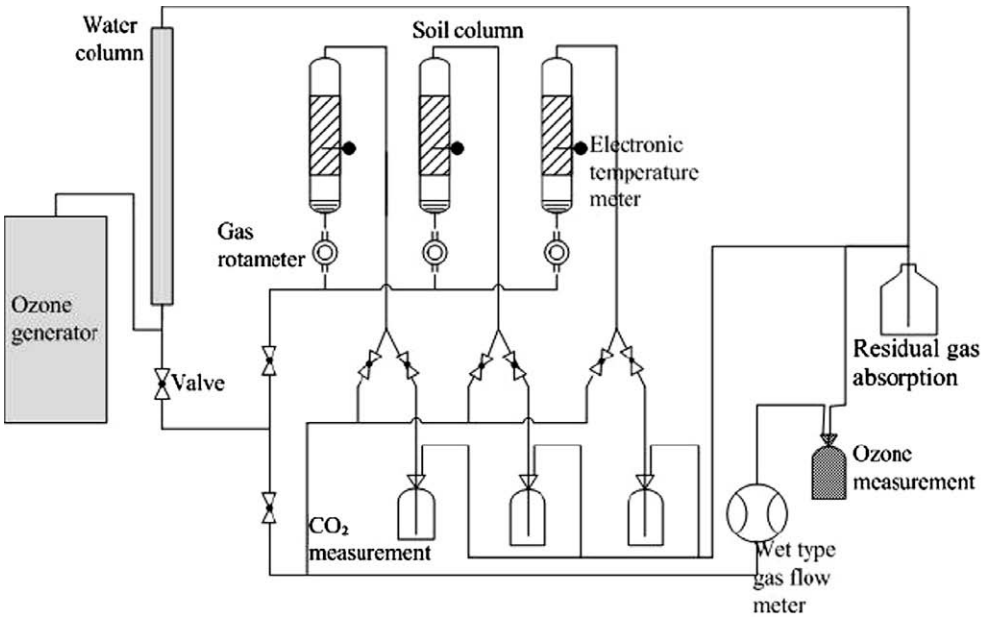

Fig. 1. Schematic of the laboratory-scale soil column experimental system.

incubated directly or after inoculation with enriched indigenous microbes as described previously. A control was set up with an equal amount of soil that had not been treated with ozone. All three treatments were incubated at room temperature and stirred every 3 d for aeration. The soil water content was maintained at 15–30%. Available nutrients were adjusted with urea and phosphate at a C/N/P ratio of 100:10:1. Biodegradation was performed for 125 d.

2.4. Crude oil extraction and analysis

The concentration of crude oil in the contaminated soil was determined using an Ultrasonic-Soxhlet extraction gravimetric method (Huesemann, 1995). The four components (aliphatic hydrocarbons, aromatic hydrocarbons, NSO fraction and asphaltenes) of crude oil were separated using silica gel (0.15–0.18 mm) and alumina (0.07–0.15 mm) column chromatography. Crude oil (approximately 50 mg) was dissolved in *n*-hexane for 12 h to precipitate asphaltene. Asphaltene was filtered with absorbent cotton then washed with chloroform. The filtrate was then transferred to the column. The aliphatic hydrocarbon, aromatic hydrocarbon and NSO fractions were washed off in sequence with *n*-hexane, a mixture of chloroform and dichloromethane (1:2), and chloroform, respectively. The amount of each component was determined by weight after the solvent was evaporated. Both the crude oil and the four components (10 μL sample volume) were analyzed with GC/MS (Thermo DSQ II Single Quadrupole) using VF-5 ms capillary columns (30.0 m × 0.25 mm × 0.25 μm). High purity nitrogen (99.99%) was used as the carrier gas. The temperature program was as follows: 100 °C for 2 min, increase to 300 °C at 5 °C min^{-1}, held for 50 min.

2.5. Microbial population analysis

The hydrocarbon-degrading bacterial populations were determined by the Most Probable Number method. Aliquots of soil (2 g) were mixed with 100 mL sterilized distilled water and incubated with shaking (150 rpm, 4 h). Then, 2 mL of suspension were serially diluted to 10^{-10} with minimal salts medium containing paraffin as the sole carbon source and incubated at 37 °C. The microbial populations were determined after 7 d.

2.6. Nucleic acid extraction, purification, amplification and labeling

The microbial whole genomic DNA was extracted from 5 g of well-mixed soil samples by combining freeze-grinding and sodium dodecyl sulfate (SDS) for cell lysis as detailed in Zhou et al. (1996). The crude DNA was purified by agarose gel electrophoresis followed by phenol–chloroform–butanol extraction. The purified DNA was quantified with an ND-1000 spectrophotometer (Nanodrop Inc.) and Quant-It PicoGreen (Invitrogen, Carlsbad, CA). An aliquot of 100 ng DNA from each sample was amplified in triplicate using the TempliPhi kit (Amersham Biosciences, Piscataway, NJ) in a modified buffer containing single strand binding protein (200 ng μL^{-1}) and spermidine (0.04 mM) to increase the sensitivity of amplification, incubating at 30 °C for 3 h (Wu et al., 2006). All of the amplified DNA was denatured by boiling for 5 min at 99.9 °C with 1 × random octamer mix (Invitrogen, Carlsbad, CA, USA) and then fluorescently labeled in a reaction solution containing 50 μM dATP, dCTP, dGTP, 20 μM dTTP (USB Corporation, Cleveland, OH), 1 mM Cy5 dUTP (Amersham Pharmacia Biotech, Piscataway, NJ), and 40 U of Klenow fragment (Invitrogen, Carlsbad, CA), incubating at 37 °C for 3 h. The labeled products were purified with a QIAquick PCR purification kit (Qiagen, Valencia, CA), dried and resuspended in 130 μL hybridization solution containing 50% formamide, 3 × saline sodium citrate buffer, 0.3% SDS, 0.7 ng μL^{-1} herring sperm DNA, 0.02 mM dithiothreitol (Invitrogen, Carlsbad, CA, USA) and water.

2.7. Microarray hybridizations, scanning and array data processing

The fluorescently labeled DNA was hybridized with GeoChip 2.0 on an HS4800 Hybridization Station (TECAN US, Durham, NC, USA) in triplicate at 42 °C for 10 h. Microarrays were scanned on a ScanArray 5000 Microarray Analysis System (Perkin–Elmer, Wellesley, MA) at 95% laser power and 68% photomultiplier tube gain as described previously (Wu et al., 2006).

Signal intensities of each spot were measured with ImaGene 6.0 (Biodiscovery Inc., El Segundo, CA, USA). Only the spots automatically scored as positive in the output raw data were used for further data analysis. The signal intensities used for final analysis were background-subtracted. Intensities of three replicates for each set of experiments were normalized using mean signal intensities (Wu et al., 2008). Spots with signal-to-noise ratios (He and Zhou, 2008) <2.0 and replicates outliers (>2 standard deviation) were removed. Gene detection was considered positive when a positive hybridization signal was obtained from $\geqslant$51% of spots targeting the gene of all replicates.

Cluster analysis was performed using the pairwise average-linkage hierarchical clustering algorithm (Eisen et al., 1998) using PC-ORD (MjM Software, Gleneden Beach, Oregon, USA).

3. Results and discussion

3.1. High-molecular weight residual contaminants in the soil

The concentration of crude oil in the long-term weathered soil from Daqing oilfield was initially approximately 56 mg g^{-1} and decreased to 28 mg g^{-1} after 242 d of laboratory-scale bioremediation. Aliphatic and aromatic hydrocarbons were the main residual components, 36.8% and 34.5%, respectively. The distribution of *n*-alkanes in the crude oil, the long-term weathered contaminated soil, and the laboratory bioremediated soil are shown in Fig. 2. The *n*-alkanes undecane (C_{11}) to dotriacontane (C_{32}) were detected in the crude oil. Low-molecular alkanes (<C_{11}) were not detected, either because these components volatilized or were biodegraded. In the weathered soil, tetradecane (C_{14}) to dotriacontane (C_{32}) were present. There was a sharp decrease of component abundance in tetradecane (C_{14}) to hexadecane (C_{16}) and an increase of 0.6–2.6% in octadecane (C_{18}) to dotriacontane (C_{32}) compared to the crude oil. The residual *n*-alkanes in the bioremediated soil consisted of pentadecane (C_{15}) to hentriacontane (C_{31}). Compared to the weathered soil, there was a decrease in pentadecane (C_{15}) to nonadecane (C_{19}), and an increase of 0.7–5.1% in tricosane (C_{23}) to hentriacontane (C_{31}). Most aromatic hydrocarbons, especially PAHs with 2–5 rings and their alkylated derivatives, were detected in both weathered and bioremediated soils in similar abundance (Table 2). Only a few compounds with relatively simple structures were below the detection limit. A large amount of PAHs remained in the soil with minimal degradation. Results of GC/MS analysis indicated that most of the residuals in the crude oil contaminated soil, even after bioremediation, were high-molecular weight compounds, such as long-chain *n*-alkanes, PAHs, and their alkylated derivatives, which are highly bio-resistant.

Table 2
Components of aromatic hydrocarbons detected by GC/MS.

Retention time (min)	Name
8.43	Benzene, 1,1′-(3,3-dimethyl-1-butenylidene)bis-[1]
8.78	1H-Indene, 2,3-dihydro-1,1,3-trimethyl-3-phenyl-
9.79	Anthracene
10.12	Benzene, 1,1′-(1,1,2,2-tetramethyl-1,2-ethanediyl)bis-
10.59	1,1′-Biphenyl, 3,4-diethyl-[1]
11.05	2,4-Diphenyl-4-methyl-2(E)-pentene
14.56	Phenanthrene, 2,3-dimethyl-
14.60	Phenanthrene, 1,7-dimethyl-
14.78	Benzene, 1,1′-ethylidenebis[4-ethyl-[1]
15.83	Pyrene
16.61	Benzene, 1,1′-ethylidenebis[4-ethyl-[1]
18.33	Pyrene, 2-methyl-
18.45	Pyrene, 1-methyl-
21.55	Benz[a]anthracene
25.77	Benzo[c]phenanthrene, 5,8-dimethyl-
26.94	Benzo[a]pyrene
29.17	Benz[j]aceanthrylene, 3-methyl-

[1] Compounds not detected in bioremediated soils.

3.2. Ozonation with subsequent biodegradation of residual contaminants

A 22% reduction in residual crude oil in the bioremediated soil occurred after a 6-h ozonation treatment (10 mg L^{-1}; flow rate of 2.0 L min^{-1}). GC/MS was used to monitor changes in the crude oil composition. The concentrations of *n*-alkanes before and after ozonation indicated that eicosane (C_{20}) to octacosane (C_{28}) decreased by 34–63%. Heptadecane (C_{17}), octadecane (C_{18}) and nonadecane (C_{19}) showed a slight decrease and tetradecane (C_{14}) and pentadecane (C_{15}) appeared. Meanwhile, ozonated polar products were generated, mainly *n*-aldehydes, tridecanaldehyde (C_{13}) to decenaldehyde (C_{20}), and monocarboxylic acids, nonanoic acid

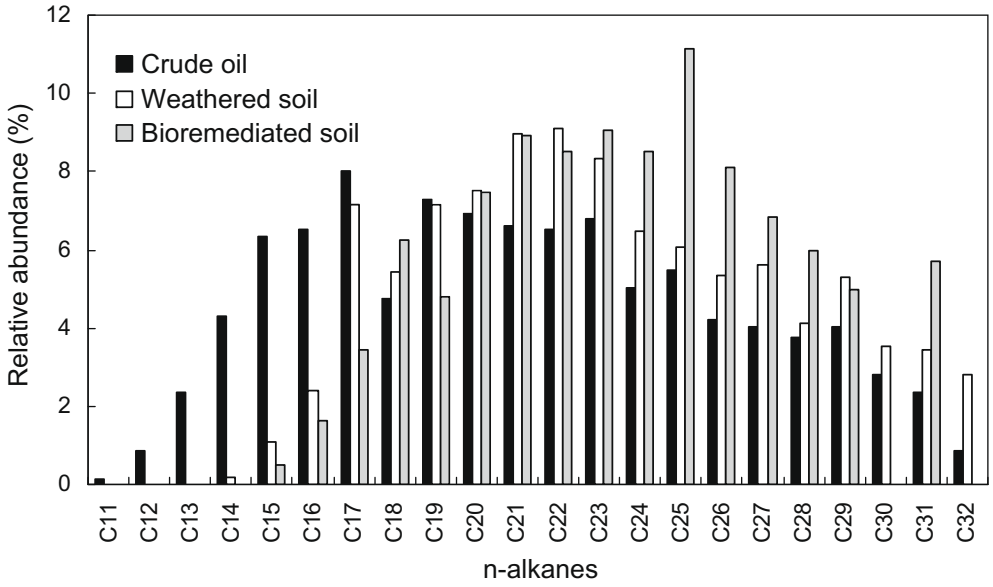

Fig. 2. *N*-alkane ($C_{11}H_{24}$–$C_{32}H_{66}$) distribution in crude oil, weathered soil and bioremediated soil determined by GC/MS.

(C_9) to eicosanoic acid (C_{20}). Lack of short-chain *n*-aldehydes may be due to further oxidation to carboxylic acids. The ozonated products such as aldehydes and acids have octanol–water partition coefficients (K_{ow}) from 10^4 to 10^7, which are more water-soluble and bioavailable than the parent compounds (K_{ow}, 10^7–10^{12}).

Ozonation of *n*-alkanes is initially by an attack of the C–H bond to generate the transient intermediate hydrotrioxide (ROOOH), which then decomposes to aldehydes, ketones and carboxylic acids (Oyama, 2000). Generally, alkanes are less reactive to direct ozone oxidation and the reaction rate constant (k) is 10^{-2} M^{-1} s^{-1} in water, while the *n*-alkanes are broken up via chain reactions with OH and k increases to 10^6–10^9 M^{-1} s^{-1} (Oyama, 2000). Ozone is much more reactive with aromatic hydrocarbons via a 1,3-dipolar cyclic addition of ozone to the double bond to form the unstable intermediate trioxalane, and then decomposition to catechols, aldehydes and carboxylic acids. The prevalent carboxylic acid is generally unreactive with ozone and can be further decomposed to CO_2 and H_2O via OH secondary oxidation. A continuous linear increase ($r^2 = 0.992$) of CO_2 during the ozonation was observed in this study. The generation of aldehydes, carboxylic acids and CO_2 confirmed the simultaneous occurrence of direct and indirect oxidation during ozonation.

Humic substances in the soil compete with crude oil contaminants during ozonation (Ohlenbusch et al., 1998). A 2.0 mg g^{-1} dry soil loss of humic substances in the soil was observed after 6 h ozonation. Steady phase humus decreased from 10.7 to 8.2 mg g^{-1} dry soil, and loose phase humus increased slightly from 6.5 to 7.0 mg g^{-1} dry soil. While humic substances cause extra ozone consumption, they could also act as catalysts to promote the production of hydroxyl radicals (Yu et al., 2007). In addition, metal oxides, which are at relatively high concentrations in crude oil contaminated soils, could catalyze hydroxyl radical reactions (Yu et al., 2007).

In the 125 d laboratory biodegradation system following ozonation, the final average crude oil concentration was 18 mg g^{-1} dry soil after direct biodegradation, 17 mg g^{-1} dry soil after bioaugmentation and remained at 25 mg g^{-1} dry soil in the control system. Approximately 12–20% of the residual crude oil was removed in the subsequent biodegradation. As shown in Fig. 3, the concentrations of aliphatic and aromatic hydrocarbons decreased 36% and 51% after ozonation, respectively, while the NSO fraction increased 11% and asphaltenes changed little. The subsequent biodegradation step decreased primarily the aromatic hydrocarbon and NSO fractions.

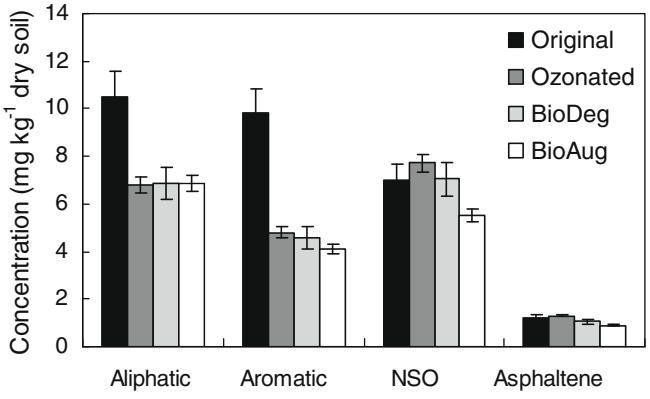

Fig. 3. Four components of crude oil (aliphatic hydrocarbons, aromatic hydrocarbons, NSO fraction and asphaltenes) in soil before ozonation (Original), after ozonation (Ozonated), direct biodegradation after ozonation (BioDeg), and bioaugmentation after ozonation (BioAug).

Table 3
Microbial diversity indices of soil before ozonation (Original), after ozonation (Ozonated), direct biodegradation after ozonation (BioDeg), and bioaugmentation after ozonation (BioAug).

Sample	Original	Ozonated	BioDeg	BioAug
Equitability (evenness)	0.929	0.919	0.905	0.896
Simpson's (1/D)	224	128	112	94
Shannon Weaver's H'	5.89	5.35	5.33	5.14

3.3. Overall functional gene diversity

Soils before and after ozonation and late in the subsequent direct biodegradation and bioaugmentation treatments were selected to examine the microbial functional gene changes using GeoChip. In total, 564 functional genes were detected in soil before ozonation and decreased to 335 after ozonation. In the direct biodegradation treatment soil, 362 genes were detected, of which 26% overlapped with genes detected in soil before ozonation and 37% were unique genes not found in the other soils. A total of 309 genes were detected in the bioaugmentation treatment, of which 22% overlapped with genes detected in soil before ozonation and 38% were unique. The functional genes detected in the original soil were evenly distributed. This did not change much after ozonation and biodegradation, as the evenness index values were all close to 1 (Table 3). Simpson's reciprocal diversity index (1/D) indicated a decrease of genetic diversity after ozonation and a further decrease following biodegradation. Similar results were also observed by using the Shannon–Weaver diversity index (Table 3). Hierarchical cluster of all functional genes indicated that the microbial functional genetic patterns were most similar before and after ozonation. The direct biodegradation and bioaugmentation treatment communities were most dissimilar from the others.

Although ozone can act as a sterilizing agent to microorganisms, in this study, the ozonation process did not cause a die-off event of hydrocarbon-degrading bacteria. The hydrocarbon-degrading bacterial population remained at 10^4 cells g^{-1} soil after ozonation and about 60% of functional genes detected in the original soil were detected after ozonation. The "non die-off" event was also reported by Jung and colleagues who observed that the numbers of heterotrophic, alkane-degrading, and phenanthrene-degrading bacteria were reduced from 10^8 to 10^4, 10^7–10^3, and 10^6 CFU g $soil^{-1}$ to below detection limit, respectively, after 900 min of ozonation (Jung et al., 2005). This phenomenon could be due to nonuniform diffusion of ozone into the soil or total depletion of ozone by reaction with contaminants or by self-decomposition before reaching the bacteria, especially those within soil micro-pores. The surviving microorganisms were adaptable to environmental conditions and had the capacity to degrade ozonated polar compounds.

3.4. Changes in microbial functional genes

To examine how ozonation and the biodegradation treatment influenced soil microbial ecological functions, functional gene changes were analyzed in detail. For most functional groups, including metal reduction, metal resistance, methane generation and oxidation, nitrogen cycling, and organic contaminant remediation, functional genes before and after ozonation clustered together. For carbon degradation and fixation groups, genes in the ozonated soil and in direct biodegradation were most similar. For sulfate reducing group, genes in ozonated soil and in the bioaugmentation soils were similar. Ozonation and subsequent biodegradation changed microbial genetic patterns varying in different functional groups.

Key genes with the highest hybridization signal intensities in each functional gene group are presented in Table 4. The normal-

Table 4
Normalized signal intensities of 25 key genes in soil before ozonation (Original), after ozonation (Ozonated), direct biodegradation after ozonation (BioDeg), and bioaugmentation after ozonation (BioAug).

Key genes	Functional category	Original	Ozonated	BioDeg	BioAug
Cellulase	Carbon degradation	20 ± 8	12 ± 4	15 ± 5	18 ± 6
Chitinase	Carbon degradation	5 ± 1	Undetected	3 ± 1	8 ± 5
Laccase	Carbon degradation	11 ± 3	5 ± 2	7 ± 2	8 ± 2
rbcL	Carbon fixation	12 ± 4	2 ± 1	8 ± 2	6 ± 2
dsr	Sulfate reduction	66 ± 20	19 ± 5	56 ± 21	20 ± 7
Cytochrome	Metal reduction	14 ± 5	2 ± 1	11 ± 6	10 ± 5
mcr	Methane generation	5 ± 1	3 ± 1	2 ± 1	1
mmo	Methane oxidation	11 ± 4	8 ± 2	11 ± 5	9 ± 3
pmo	Methane oxidation	6 ± 2	5 ± 2	6 ± 3	6 ± 2
nifH	Nitrogen fixation	11 ± 3	4 ± 1	10 ± 3	6 ± 2
Urease	Nitrification	67 ± 17	31 ± 8	45 ± 16	31 ± 7
narG	Nitrogen reduction	16 ± 4	7 ± 2	13 ± 5	11 ± 3
nasA	Nitrogen reduction	22 ± 7	17 ± 5	13 ± 2	13 ± 4
nir	Nitrogen reduction	25 ± 7	11 ± 3	6 ± 2	13 ± 5
norB	Nitrogen reduction	9 ± 2	1	15 ± 7	8 ± 1
nosZ	Nitrogen reduction	10 ± 2	8 ± 2	5 ± 1	4 ± 1
Catechol	Organic contaminant degradation	26 ± 7	7 ± 2	26 ± 9	21 ± 6
Protocatechuate	Organic contaminant degradation	26 ± 11	27 ± 10	30 ± 11	15 ± 7
Benzoate	Organic contaminant degradation	31 ± 12	24 ± 7	11 ± 4	21 ± 7
Phthalate	Organic contaminant degradation	12 ± 8	9 ± 3	12 ± 7	10 ± 7
Benzene	Organic contaminant degradation	7 ± 2	1	3 ± 1	17 ± 1
Xylene	Organic contaminant degradation	3 ± 1	Undetected	2 ± 1	1
Biphenyl	Organic contaminant degradation	8 ± 3	2 ± 1	5 ± 2	3 ± 1
Naphthalene	Organic contaminant degradation	7 ± 2	Undetected	2 ± 1	1
Pyrene	Organic contaminant degradation	9 ± 2	11	8 ± 1	7

ized total signal intensities provide a quantitative measurement of environmental microbial gene densities (Rhee et al., 2004; He et al., 2007; Wu et al., 2008). The carbon degradation genes encoding cellulase, chitinase and laccase decreased after ozonation, by 40% for cellulase, 54% for laccase and below detection for chitinase. All of these genes recovered in the subsequent biodegradation process, with cellulase returning to its original level and an even higher abundance of chitinase after bioaugmentation. The cellulase genes derived mainly from *Mycobacterium*-like, *Pectobacterium*-like and *Mesorhizobium*-like throughout. The chitinase genes derived mainly from *Streptomyces*-like before ozonation, and shifted to *Neurospora*-like during direct biodegradation and to *Burkholderia*-like and an uncultured bacterium (chitinase 18182596, protein gi in the National Center for Biotechnology Information database, same in the following) during bioaugmentation. The dominant bacteria with laccase-encoding genes shifted from *Pleurotus*-like to *Piloderma*-like during both direct biodegradation and bioaugmentation. The *rbcL* gene pertaining to carbon fixation decreased by 80% after ozonation but showed some recovery after biodegradation. The *rbcL* gene derived mainly from an uncultured bacterium (*rbcL* 21038746) before ozonation and during direct biodegradation, and shifted to another uncultured bacterium (*rbcL* 7592883) during bioaugmentation.

The sulfate reduction *dsr* genes decreased 71% after ozonation and had a high recovery during direct biodegradation. A high abundance of a *dsr* gene from an uncultured bacterium (*dsr* 20501985) before ozonation shifted to *dsr* (30525370) and *dsr* (30525455) during direct biodegradation. The cytochrome genes involved in metal reduction decreased by 84% after ozonation and recovered to about 80% after direct biodegradation and bioaugmentation. The dominant populations were *Rhodopseudomonas*-like before ozonation and during direct biodegradation and *Geobacter*-like during bioaugmentation. The *mcr* genes pertaining to methane generation showed a continuous decrease. The population primarily derived from *Methanothermobacter*-like and *Methanopyrus*-like throughout except after bioaugmentation. Methane oxidation genes appeared to be more stable, especially the *pmo* genes, which were derived mainly from *Methylococcus*-like, *Methylocystis*-like and *Methylosinus*-like.

The *nifH* and urease genes decreased by 61% and 54%, respectively, after ozonation and showed recovery after direct biodegradation and slightly less recovery after bioaugmentation. The dominant *nifH* genes derived from uncultured bacterium (*nifH* 20278769) throughout and with *nifH* (29293350) unique to before ozonation. The urease genes mainly derived from *Brucella*-like throughout and *Mesorhizobium*-like except in bioaugmentation. *Bacillus sp.* was unique after direct biodegradation. The *narG*, *nasA*, *nir*, *norB*, *nosZ* genes pertaining to nitrogen reduction decreased after ozonation, ranging from 23% to 87%. The dominant bacteria coding *narG* genes shifted from *Paracoccus*-like before ozonation to uncultured bacterium (*narG* 26278814) after direct biodegradation and uncultured bacterium (*narG* 29652556) after bioaugmentation. The *nasA* genes derived from *Sphingomonas*-like were dominant throughout. The *nir* genes derived mainly from *Alcaligenes*-like and uncultured bacterium (*nir* 24528386) before and uncultured bacterium (*nir* 24415232) after direct biodegradation and uncultured bacterium (*nir* 38455924) after bioaugmentation. The dominant bacteria coding *norB* genes were *Achromobacter*-like and *Nitrosococcus*-like before ozonation and shifted to uncultured bacterium (*norB* 29465998) after both direct biodegradation and bioaugmentation. The *nosZ* genes derived mainly from *Paracoccus*-like before ozonation and after direct biodegradation and derived from uncultured bacterium (*nosZ* 4633572) before ozonation and after bioaugmentation.

For organic contaminant degradation, catechol is a key dihydroxylated intermediate in the PAH catabolic pathways. Catechol can be cleaved by dioxygenase *via* either an *ortho*-cleavage pathway or a *meta*-cleavage pathway to the tricarboxylic acid cycle (Habe and Omori, 2003). The catechol genes decreased 72% after ozonation and recovered after both the direct biodegradation and bioaugmentation treatments. The genes derived mainly from unidentified bacterium (catechol 3402328, 3402316), *Comamonas*-like and *Wautersia*-like before ozonation, and *Mycobacterium*-like, *Ralstonia*-like and *Rhodopseudomonas*-like after direct biodegradation and uncultured bacterium (catechol 28556672) and *Ralstonia*-like after bioaugmentation. The protocatechuate genes remained stable except for a decrease after bioaugmentation. These genes mainly derived from *Rhodobacter*-like and

Sinorhizobium-like throughout. Most genes involved in degrading benzonate, phthalate, benzene, xylene, biphenyl, naphthalene and pyrene, decreased and then recovered after both direct biodegradation and bioaugmentation.

Among the 25 key gene families for carbon degradation and fixation, nitrogen cycling, sulfate reduction, methane generation and oxidation, metal reduction and organic contaminant degradation, most recovered to some extent during direct biodegradation and bioaugmentation after a sharp decrease following ozonation. As reported by Jung and colleagues (2005), three types of indigenous microbes (heterotrophic microbes, alkane-degrading microbes and phenanthrene-degrading microbes) had different sensitivities to ozone exposure. Also in this study, microbial functional genes presented different responses to ozone exposure and showed differing recovery capacities, which may be due to their soil niche characteristics (Ahn et al., 2005).

4. Conclusions

In summary, ozonation treatment removed a large amount of high-molecular weight residual contaminants, promoting further degradation. The resulting ozonated products, such as *n*-aldehydes and *n*-monocarboxylic acids were more biodegradable as demonstrated by reduction in these components after direct biodegradation and bioaugmentation. Although microbial functional gene numbers and diversity decreased after ozonation, most key functional genes recovered during the subsequent biodegradation, indicating the potential of functional recovery for microbes involved in the ecological processes of carbon, nitrogen, sulfur cycling, metal reduction and resistance, and organic contaminant remediation. These results provide a detailed profile of crude oil component changes and the response of microbial communities and their functional genes during the integrated ozonation and biodegradation treatments, indicating the potential of this approach in the field.

Acknowledgements

This work was supported by the National Natural Scientific Foundation of China (No. 40730738), and by the United States Department of Energy under the Genomics: GTL program through the Virtual Institute of Microbial Stress and Survival (VIMSS; http://vimss.lbl.gov), and the Environmental Remediation Science Program.

References

Ahn, Y., Jung, H., Tatavarty, R., Choi, H., Yang, J.W., Kim, I.S., 2005. Monitoring of petroleum hydrocarbon degradative potential of indigenous microorganisms in ozonated soil. Biodegradation 16, 45–56.

Angehrn, D., Gälli, R., Zeyer, J., 1998. Physicochemical characterization of residual mineral oil contaminants in bioremediated soil. Environ. Toxicol. Chem. 17, 2168–2175.

Chaineau, C.H., Morel, J.L., Oudot, J., 1995. Microbial-degradation in soil microcosms of fuel-oil hydrocarbons from drilling cuttings. Environ. Sci. Technol. 29, 1615–1621.

Eisen, M.B., Spellman, P.T., Brown, P.O., Botstein, D., 1998. Cluster analysis and display of genome-wide expression patterns. Prog. Natl. Acad. Sci. USA 95, 14863–14868.

Ferrarese, E., Andreottola, G., Oprea, I.A., 2008. Remediation of PAH-contaminated sediments by chemical oxidation. J. Hazard. Mater. 152, 128–139.

Habe, H., Omori, T., 2003. Genetics of polycyclic aromatic hydrocarbon metabolism in diverse aerobic bacteria. Biosci. Biotech. Biochem. 67, 225–243.

He, Z., Gentry, T.J., Schadt, C.W., Wu, L., Liebich, J., Chong, S.C., Huang, Z., Wu, W., Jardine, P., Criddle, C., Zhou, J., 2007. GeoChip: a comprehensive microarray for investigating biogeochemical, ecological and environmental processes. ISME J. 1, 67–77.

He, Z., Zhou, J., 2008. Empirical evaluation of a new method for calculating signal-to-noise ratio for microarray data analysis. Appl. Environ. Microb. 74, 2957–2966.

Huesemann, M.H., 1995. Predictive model for estimating the extent of petroleum hydrocarbon biodegradation in contaminated soils. Environ. Sci. Technol. 29, 7–18.

Ivancev-Tumbas, I., Trickovic, J., Karlovic, E., Tamas, Z., Roncevic, S., Dalmacija, B., Petrovic, O., Klasnja, M., 2004. GC/MS-scan to follow the fate of crude oil components in bioreactors set to remediate contaminated soil. Int. Biodeter. Biodegrad. 54, 311–318.

Jung, H., Ahn, Y., Choi, H., Kim, I.S., 2005. Effects of in situ ozonation on indigenous microorganisms in diesel contaminated soil: survival and regrowth. Chemosphere 61, 923–932.

Kulik, N., Goi, A., Trapido, M., Tuhkanen, T., 2006. Degradation of polycyclic aromatic hydrocarbons by combined chemical pre-oxidation and bioremediation in creosote contaminated soil. J. Environ. Manage. 78, 382–391.

Li, X., He, Z., Zhou, J., 2005. Selection of optimal oligonucleotide probes for microarrays using multiple criteria, global alignment and parameter estimation. Nucl. Acid Res. 33, 6114–6123.

Lu, R.K., 1999. Soil Agricultural Chemical Analysis. China Agricultural Science and Technology Press, Nanjing.

Nam, K., Kukor, J.J., 2000. Combined ozonation and biodegradation for remediation of mixtures of polycyclic aromatic hydrocarbons in soil. Biodegradation 11, 1–9.

Nocentini, M., Pinelli, D., Fava, F., 2000. Bioremediation of a soil contaminated by hydrocarbon mixtures: the residual concentration problem. Chemosphere 41, 1115–1123.

O'Mahony, M.M., Dobson, A.D.W., Barnes, J.D., Singleton, I., 2006. The use of ozone in the remediation of polycyclic aromatic hydrocarbon contaminated soil. Chemosphere 63, 307–314.

Ohlenbusch, G., Hesse, S., Frimmel, F.H., 1998. Effects of ozone treatment on the soil organic matter on contaminated sites. Chemosphere 37, 1557–1569.

Oyama, S.T., 2000. Chemical and catalytic properties of ozone. Catal. Rev. 42, 279–322.

Rhee, S., Liu, X., Wu, L., Chong, S., Wan, X., Zhou, J., 2004. Detection of genes involved in biodegradation and biotransformation in microbial communities by using 50-mer oligonucleotide microarrays. Appl. Environ. Microb. 70, 4303–4317.

Rivas, F.J., 2006. Polycyclic aromatic hydrocarbons sorbed on soils: a short review of chemical oxidation based treatments. J. Hazard. Mater. 138, 234–251.

Romantschuk, M., Sarand, I., Petanen, T., Peltola, R., Jonsson-Vihanne, M., Koivula, T., Yrjälä, K., Haahtela, K., 2000. Means to improve the effect of in situ bioremediation of contaminated soil: an overview of novel approaches. Environ. Pollut. 107, 179–185.

Semple, K.T., Morriss, A.W.J., Paton, G.I., 2003. Bioavailability of hydrophobic organic contaminants in soils: fundamental concepts and techniques for analysis. Eur. J. Soil Sci. 54, 809–818.

Sung, M., Lee, S.Z., Huang, C.P., 2008. Ozonation of pentachlorophenol in unsaturated soils. J. Contam. Hydrol. 98, 75–84.

Wu, L., Kellogg, L., Devol, A.H., Tiedje, J.M., Zhou, J., 2008. Microarray-based characterization of microbial community functional structure and heterogeneity in marine sediments from the Gulf of Mexico. Appl. Environ. Microb. 74, 4516–4529.

Wu, L., Liu, X., Schadt, C.W., Zhou, J., 2006. Microarray-based analysis of subnanogram quantities of microbial community DNAs by using whole-community genome amplification. Appl. Environ. Microb. 72, 4931–4941.

Yergeau, E., Kang, S., He, Z., Zhou, J., Kowalchuk, G., 2007. Functional microarray analysis of nitrogen and carbon cycling genes across an Antarctic latitudinal transect. ISME J. 1, 163–179.

Yu, D.Y., Kang, N., Bae, W., Banks, M.K., 2007. Characteristics in oxidative degradation by ozone for saturated hydrocarbons in soil contaminated with diesel fuel. Chemosphere 66, 799–807.

Yu, X., Li, L., Gao, J., Cheng, S., 2001. Analysis for total amount of multielement in soil by ICP-AES. Mod. Instr. 2, 30–32.

Zhou, J., Bruns, M., Tiedje, J.M., 1996. DNA recovery from soils of diverse composition. Appl. Environ. Microb. 62, 316–322.

Zhou, J., Kang, S., Schadt, C.W., Garten, C.T., 2008. Spatial scaling of functional gene diversity across various microbial taxa. Prog. Natl. Acad. Sci. USA 105, 7768–7773.